Preprints.org

Article

Not peer-reviewed version

A Chimeric Vaccine Based on a Single Fusion Protein (W-PreS-O) Combining RBDs from Wuhan hu-1 Wild Type and Omicron Shows Protective Effect against Omicron Infection in Syrian Hamsters

Pia Gattinger , Liubov I. Kozlovskaya , Aleksandr Lunin , Olga S. Gancharova , Dina I. Sirazova , Vasiliy Apolokhov , Egor S. Chekina , Ilya Gordeychuk , Alexander Karaulov , Rudolf Valenta * , Aydar Ishmukhametov

Posted Date: 29 May 2024

doi: 10.20944/preprints202405.1895.v1

Keywords: SARS-CoV-2; COVID-19; Omicron; vaccine; neutralizing antibodies; infection model; Syrian hamster

Preprints.org is a free multidiscipline platform providing preprint service that is dedicated to making early versions of research outputs permanently available and citable. Preprints posted at Preprints.org appear in Web of Science, Crossref, Google Scholar, Scilit, Europe PMC.

Copyright: This is an open access article distributed under the Creative Commons Attribution License which permits unrestricted use, distribution, and reproduction in any medium, provided the original work is properly cited.

Preprints.org (www.preprints.org) | NOT PEER-REVIEWED | Posted: 29 May 2024 doi:10.20944/preprints202405.1895.v1

Disclaimer/Publisher's Note: The statements, opinions, and data contained in all publications are solely those of the individual author(s) and contributor(s) and not of MDPI and/or the editor(s). MDPI and/or the editor(s) disclaim responsibility for any injury to people or property resulting from any ideas, methods, instructions, or products referred to in the content.

Article

A Chimeric Vaccine Based on a Single Fusion Protein (W-PreS-O) Combining RBDs from Wuhan hu-1 Wild Type and Omicron Shows Protective Effect against Omicron Infection in Syrian Hamsters

Pia Gattinger [1,†], Luibov I. Kozlovskaya [2,†], Alexander S. Lunin [2], Olga S. Gancharova [2], Dina I. Sirazova [2,3], Vasiliy D. Apolokhov [2], Egor S. Chekina [2], Ilya V. Gordeychuk [2,3], Alexander V. Karaulov [4] and Rudolf Valenta [1,4,5,6,*] and Aydar A. Ishmukhametov [2,3,*]

1 Medical University of Vienna, Center for Pathophysiology, Infectiology and Immunology, Department of Pathophysiology and Allergy Research, Division of Immunopathology, 1090 Vienna, Austria;
2 Chumakov Federal Scientific Center for Research and Development of Immune-and-Biological Products of Russian Academy of Sciences, Institute of Poliomyelitis, 108819 Moscow, Russia
3 Sechenov First Moscow State Medical University, Institute for Translational Medicine and Biotechnology, 119048 Moscow, Russia
4 Sechenov First Moscow State Medical University,Laboratory for Immunopathology, Department of Clinical Immunology and Allergology, 119048 Moscow, Russia
5 Karl Landsteiner University of Health Sciences, 3500 Krems, Austria;
6 NRC Institute of Immunology FMBA of Russia, Moscow, Russia
* Correspondence: rudolf.valenta@meduniwien.ac.at, ishmukhametov@chumakovs.su
† Contributed equally

Abstract: Omicron SARS-CoV-2 variants have dominated the strains of COVID-19 circulating worldwide for the last two years. Although the mortality rate of the COVID-19 Omicron variants is only approximately half that of previous variants, vaccines effective against Omicron are needed. Demonstrating that a SARS-CoV-2 vaccine can protect against Omicron in an in vivo infection model, particularly in that of Syrian hamsters, is important for the preclinical characterization of SARS-CoV-2 vaccines. Here, we report on the evaluation of W-PreS-O for its ability to protect Syrian hamsters against infection by Omicron. W-PreS-O is a chimeric vaccine based on a single fusion protein (W-PreS-O), combining RBDs from Wuhan hu-1 wild-type and Omicron adsorbed to aluminum hydroxide. The Syrian hamsters were immunized three times at three-week intervals with W-PreS-O or with aluminum hydroxide (placebo), and then they were infected with Omicron BA.1. Non-infected and non-vaccinated animals served as controls. Neutralizing antibody (nAB) titers, weight, lung symptoms (i.e., edema and pneumonia index), and viral loads, as measured using RT-PCR in the upper and lower respiratory tracts, were determined. In addition, infectious virus titers from the lungs were measured using a plaque-forming assay. W-PreS-O-vaccinated hamsters developed robust nABs against Omicron, showed almost no development of pneumonia, and had significantly reduced infectious virus titers in the lungs. Importantly, the viral loads in the nasal cavities of W-PreS-O-vaccinated hamsters were close to or above the PCR cycle threshold considered to be non-infectious. Our data provide compelling evidence demonstrating that the W-PreS-O vaccine has protective effect against Omicron in a Syrian hamster in vivo infection model. W-PreS-O is therefore a highly promising candidate vaccine for Omicron infections, and it should be further evaluated in clinical studies.

Keywords: SARS-CoV-2; COVID-19; Omicron; vaccine; neutralizing antibodies; infection model; Syrian hamster

1. Introduction

Severe acute respiratory syndrome corona virus-2 (SARS-CoV-2), the causative agent of COVID-19, became endemic approximately four years after its pandemic outbreak in late 2019 [1-3]. At present, the severity of COVID-19 symptoms in the general population is lower than at the beginning of the pandemic [4,5]. However, COVID-19 remains a major health issue, and it can present with high disease severity and mortality in vulnerable patient groups [6-8]. At least two mutually non-exclusive

© 2024 by the author(s). Distributed under a Creative Commons CC BY license.

Preprints.org (www.preprints.org) | NOT PEER-REVIEWED | Posted: 29 May 2024 doi:10.20944/preprints202405.1895.v1

explanations for the lower severity of COVID-19 in the general population may be considered. One possibility is that pre-existing immunity caused by previous infections or vaccinations has been established and that mitigates recurrent infections and disease severity [9,10]. The other explanation for the lower severity and mortality of COVID-19 is that the currently predominating variant Omicron, which differs substantially in the amino acid sequence of the spike protein and in its receptor binding domain (RBD) compared to the ancestral SARS-CoV-2 strain, is less pathogenic [11-13]. The SARS-CoV-2 variant B.1.1.529, now termed Omicron, was announced by the World Health Organization on November 24, 2021, and it appears to have an increased risk of infectivity. However, a recent meta-analysis of reports regarding disease severity concluded that the mortality rates of patients infected by Omicron ranges from 0.01% to 13.1%, while in patients infected with previous variants it was 0.08% to 29.1% [14]. Thus, the mortality rates of Omicron-induced COVID-19 seem to be at least 50% lower than for COVID-19 induced by previous variants. Nevertheless, Omicron-induced infections remain an important problem, and higher infectivity has been reported for Omicron [12,15,16]. Furthermore, SARS-CoV-2 Omicron can easily escape the immunity established by infection with previous variants and vaccines based on previous SARS-CoV-2 variants [17-20].

Accordingly, the development of vaccines for Omicron and its currently dominating and closely related sub-variants is of high priority [21-24]. Alongside the induction of cellular immune responses, like cytotoxic T cells that kill infected cells, it has become clear that antibodies specific to the spike protein S of SARS-CoV-2, and especially against its RBD, are important for protection [25,26]. However, protection requires not only high levels of specific antibodies but also a sufficient breadth of antibody response and, in particular, a high virus-neutralizing capacity. For the measurement of neutralizing antibodies (nABs), a panel of in vitro test systems has become available [27,28].

In order to evaluate protective effects of a vaccine candidate, the sole induction of nAbs alone does not seem to be sufficient. Vaccine candidates should be also evaluated in animal infection models to obtain further evidence of protective activity in vivo. The selection of an animal infection model should follow several criteria, including (i.) enabling the replication of the virus, (ii.) having a route of transmission similar to that in humans, (iii.) manifesting measurable signs of pathogenesis comparable to those in humans, and (iv.) enabling the measurement of virus-specific immune responses [29,30].

There is common agreement that the aforementioned requirements are met by Syrian hamsters, which have been used to study viral infections for more than 60 years [31]. The Syrian hamster model has been used as a successful infection model for respiratory infectious diseases caused by Severe Acute Respiratory Corona Virus (SARS) and influenza virus [29,31-33], but may not fully mimic all aspects of human mucosal immunity. It was therefore not surprising that the Syrian hamster model was identified as a conclusive infection model for SARS-CoV-2. First, the expression of the angiotensin-converting enzyme 2 (ACE2) receptor in the Syrian hamster allows for the infection of cells and viral replication. Second, Syrian hamsters become infected by SARS-CoV-2 via the upper respiratory tract, and then the virus is detectable in the lungs and respiratory system from one to five days after infection [34,35]. Third, in humans, one of the major severe COVID-19 symptoms is pneumonia [1,2,36] and, likewise, Syrian hamsters develop moderate-to-severe pulmonary lesions after infection with SARS-CoV-2 [37]. Usually, the virus is cleared after approximately 7 days [29].

Interestingly, the SARS-CoV-2 Omicron variant has also been shown to cause milder symptoms than ancestral strains in Syrian hamsters, but suitable models have been established for Omicron in Syrian hamsters [38-40]. Omicron causes less weight loss and lower viral loads in the respiratory tract than the original Wuhan strain [39]. Despite the undisputed usefulness and availability of the Syrian hamster model for Omicron, relatively few studies have been conducted to evaluate the currently registered COVID-19 vaccines that have been updated for Omicron for various reasons [41].

Here, we report on the design and characterization of a SARS-CoV-2 subunit vaccine candidate based on a fusion protein of two RBDs fused to the hepatitis B (HBV) surface antigen PreS [42]. PreS, which comprises preS1 and preS2 of the large hepatitis B virus envelope protein (LHB), has been used as a carrier protein to enhance the immunogenicity of hypoallergenic allergen peptides used in recombinant allergy vaccines [43]. In the aforementioned SARS-CoV-2 vaccine, PreS was also used to enhance the immunogenicity of the PreS-fused RBD domains. Since PreS contains the binding site of HBV to its receptor, the sodium-taurocholate co-transporting polypeptide (NTCP), on liver cells, PreS-containing vaccines induce antibodies that can protect against HBV infections [44]. The PreS-

Preprints.org (www.preprints.org) | NOT PEER-REVIEWED | Posted: 29 May 2024 doi:10.20944/preprints202405.1895.v1

based SARS-CoV-2 vaccine has been recently further developed and compared with vaccines containing fusion proteins of two RBDs from Omicron fused to PreS, and one chimeric vaccine containing a fusion protein consisting of one RBD from Wuhan and one from Omicron, termed W-PreS-O [24]. While all vaccines tested in the latter study induced comparable RBD Wuhan and RBD Omicron-specific antibody levels, the chimeric W-PreS-O (Figure 1a) showed a superior capacity to induce Omicron-neutralizing antibodies [24]. In fact, the W-PreS-O induced 7-fold higher virus-neutralizing titers (VNTs) than the wild-type-specific vaccine (e.g., W-PreS-W) and 2-fold higher VNTs to Omicron than the Omicron-specific vaccine candidate (e.g., O-PreS-O). In this study, we investigated whether the superior vaccine candidate, W-PreS-O, shows protective effects in vivo against SARS-CoV-2 Omicron infections in Syrian hamsters.

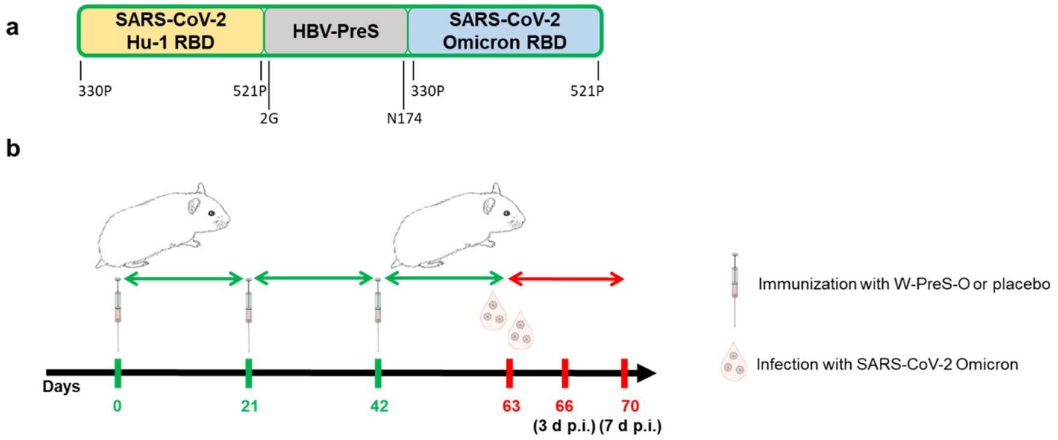

Figure 1. Schematic representation of **(a)** the recombinant fusion protein W-PreS-O, comprising RBDs from SARS-CoV- 2 Hu-1 (yellow) and Omicron BA.1 (blue), fused to the HBV-surface antigen PreS (grey). **(b)** Immunization schedule (W-PreS-O: n=16; Placebo: n=16) and infection model for the Syrian hamsters. Days post-infection = d.p.i.

2. Materials and Methods

21. Cells and Viruses

The Vero cell line was obtained from Biologicals, World Health Organization, Switzerland, and maintained in Dulbecco's Modified Eagle Medium (DMEM, Chumakov FSC R&D IBP RAS, Moscow, Russia), supplemented with 5% fetal bovine serum (FBS) (Gibco, Thermo Fisher, Waltham, MA, USA), streptomycin (0.1 mg/ml), and penicillin (100 units/ml) (both PanEco, Moscow, Russia).

The SARS-CoV-2 variant Omicron strain 7995o (Pango lineage BA.1-like, GISAID EPI_ISL_9613539) was stored as an infected cell suspension at –70 °C.

2.2. Immunization of Animals and Infection Model

In a previous study we found that W-PreS-O was more effective in inducing Omicron-neutralizing antibodies than O-PreS-O, W-PreS-W, and a mix of O-PreS-O and W-PreS-W [24]. Therefore, W-PreS-O was selected a candidate vaccine to be tested in the Syrian hamster model for its ability to induce in vivo protective antibody responses. This study was designed to compare the aluminum hydroxide-adsorbed W-PreS-O vaccine with an adequate placebo preparation (i.e., aluminum hydroxide alone). Recombinant fusion protein W-PreS-O (Figure 1a), comprising Hepatitis B virus (HBV) PreS with a N-terminal RBD from SARS-CoV-2 strain Hu-1 (Genbank accession Nr.: QHD43416.1) and a C-terminal RBD from SARS-CoV-2 variant Omicron (Pango B.1.1.529), was expressed in HEK293F cells (ThermoFisher, Waltham, MA, USA) and purified as previously described [24,42]. W-PreS-O was adsorbed onto aluminum hydroxide (SERVA Electrophoresis, Heidelberg, Germany) as described [24]. The final doses of the 150 µl vaccine formulation contained 40 µg W-PreS-O, 0.6 mg/ml aluminum hydroxide in 10 mM NaH_2PO_4, 0.9% NaCl, pH 7.2. Formulations containing 150 µl per dose of 0.6 mg/ml aluminum hydroxide in 10 mM NaH_2PO_4, 0.9% NaCl, pH 7.2, served as the placebo control.

Preprints.org (www.preprints.org) | NOT PEER-REVIEWED | Posted: 29 May 2024 doi:10.20944/preprints202405.1895.v1

Outbred Syrian hamsters (*Mesocricetus auratus*), males, 35–40 g (4 weeks old), were purchased from the Scientific Center of Biomedical Technologies, branch Stolbovaya, Russia. Randomization of animals was performed by weight into groups: intact (n = 4), placebo (n = 16), and vaccine (n = 16). The placebo and vaccine group animals were immunized intramuscularly (in the upper third of the hind limb) three times at 21-day intervals with 150 µl of the placebo or vaccine preparation per dose (Figure 1b). The placebo and vaccine group animals were infected intra-nasally with 10^4 $TCID_{50}$ (25 µL into each nostril) of the SARS-CoV-2 variant Omicron (strain 7995o) 21 days after the third vaccination. The strain used for infection (i.e., strain 7995o) differed in only one conservative exchange in the RBD from the BA.1 variant used for the vaccine design (Figure S1). The amino acid sequence of the complete W-PreS-O vaccine antigen can be found in Figure S2.

The animals were observed daily, weighed, and oropharyngeal swabs were collected. Eight animals from each infected group were euthanized on day 3 and day 7 post-infection, respectively (d.p.i.) (Figure 1b). The lungs and nasal cavities were collected and frozen for further investigation. Blood samples were collected before each vaccination and at each euthanasia point; serum samples were stored at -20 °C for neutralization tests. Since the main goal of this study was to compare the vaccinated with the non-vaccinated (i.e., placebo-treated) animals, the animals from the "intact group" were neither immunized nor infected and served as only as controls to ensure that the infection occurred in a specific manner.

The animal study protocol was approved by the Ethics Committee of the Chumakov FSC R&D IBP RAS (Protocol 190722-2, dated 19.06.22). The animals were maintained in accordance with the Directive of the European Parliament and of the Council 2010/63/ EU dated September 22, 2010 on the protection of animals used for scientific purposes.

2.3. Determination of Viral Loads

Homogenization of organs with physiological saline buffer was performed using a TissueLyser (Qiagen, Venlo, Netherlands). Swabs and organ suspensions were examined for the presence of viral RNA using POLYVIR SARS-CoV-2 (Lytech, Moscow, Russia), according to the manufacturer's protocol. Semi-quantitative results are given as cycle threshold (Ct values). The viral load in the lung suspensions was determined via titration in Vero cells. For this purpose, ten-fold dilutions of organ suspensions were prepared in DMEM (Chumakov FSC R&D IBP RAS, Moscow, Russia) and added to confluent Vero cell monolayers on 24-well plates. After 1 h of incubation at 37 °C for virus adsorption, the wells were overlaid with 1.5% methylcellulose (Sigma, Burlington, MA, USA) on DMEM containing 2% FBS. After 5 days of incubation at 37 °C, the cells were fixed with 96% ethanol and stained with 0.4% crystal violet. Plaques were counted visually, and the virus titers were expressed as plaque forming units (PFU) per gram of infected tissue (logPFU/g).

2.4. Virus Neutralization Test

Serum samples were diluted (two-fold, starting from 1:8) in DMEM and mixed with equal volumes of virus, containing in total 50–200 $CCID_{50}$ per well. After an incubation period of 1 hour at 37 °C, the serum–virus mixtures were added, in two replicates each, to confluent Vero cell monolayers. As controls, non-immune and standard immune control sera were used, and a virus dose titration was performed. The controls were performed in parallel to the serum samples derived from the animals. After five days of incubation at 37 °C, the cytopathic effect (CPE) was visually assessed via light microscopy. Antibody titers were calculated according to Kärber [45]. Results of <1:8 were considered negative (0).

2.5. Histological Examination

Lung samples were fixed for 48 hours at room temperature in 10% neutral buffered formalin, and after dehydration in isopropyl alcohol, the samples were embedded in paraffin medium. Subsequently, two micrometer-thick cross-sections from all lung lobes (two sections for each tissue block) were obtained, and representative sections were stained with Mayer's hematoxylin and hydroalcoholic eosin (both Biovitrum, Moscow, Russia) using Leica ST5010 AXL autostainer (Leica, Wetzlar, Germany). Histological preparations were converted into a digital format using a KF-PRO-400 histological scanner (KFBio, Zhejiang, China). The resulting digital versions of the histological preparations were examined using a Leica Aperio Imagescope (Leica, Wetzlar, Germany) and K-

Preprints.org (www.preprints.org) | NOT PEER-REVIEWED | Posted: 29 May 2024 doi:10.20944/preprints202405.1895.v1

Viewer software (IQM, Oslo, Norway). Representative microphotographs were obtained using the snapshot tool in the indicated software. The severity of the pathological process (pneumonia signs, including inflammation, presence of fibrinous exudate in the alveoli, loss of alveolar pattern) in the lungs of each animal was assessed according to the pneumonia intensity score (0–4), where the signs of pathological processes were rated as follows: 0—are not visible, 1—mildly pronounced, 2—moderately pronounced, 3—sharply pronounced, and 4—extremely pronounced. We also visually assessed the area of the lung tissue involvement with pathological processes (area of lung lesions) as the pneumonia area score (0–4), where 0—no changes or the lesion involved less than 10% of the area; 1—lesion involved 10–25% of the area; 2—lesion involved 25–50% of the area; 3—lesion involved 50–75% of the area; and 4—lesion involved 75–100% of the area. The results of the semi-quantitative scoring, i.e., pneumonia area score and pneumonia intensity score, were multiplied to obtain the pneumonia index for each individual lung slide (two per animal).

2.6. Statistical Analysis

Differences in antibody titers and Ct-values were determined using the Mann–Whitney test, and the weight curves were compared using an ANOVA with OriginPro Version 8 (OriginLab, Northampton, MA, USA). P values < 0.05 were considered significant.

3. Results

3.1. Immunization with W-PreS-O induces SARS-CoV-2 Omicron-Neutralizing Antibody Titers in Syrian Hamsters

The geometric mean titers (GMTs) of SARS-CoV-2 Omicron BA.1-neutralizing antibody (nAb) titers seven days after the third immunization (day 49) in the animals immunized with the W-PreS-O vaccine were 10 (median: 11, min: 0, max: 128) (Figure 2a). They further increased to mean nAB titers of 23 (median: 27, min: 0, max: 512) when measured in samples obtained on day 63, three weeks after the third immunization (Figure 2a). No nABs were detected in sera from the placebo-treated animals (Figure 2a) or in sera from the “intact group” (Supplemental Table S1) until day 63. On day 63, the animals were challenged intra-nasally with the SARS-CoV-2 Omicron strain. Three days post-virus inoculation, no relevant further increase in nAB titers in the W-PreS-O vaccine group was observed, with a GMT of 23 (median: 27). At this time point, no nABs were found in the placebo group (Figure 2a, Supplemental Table S1) or the intact group (Supplemental Table S1). The nAb response in the vaccinated animals was strongly enhanced by Omicron infection. In the vaccinated group, all but one animal, which already had a nAb titer of 512, increased their nAb titers to 1024 or higher, while only two out of eight animals in the placebo group reached a titer of 1024 through the challenge infection by seven days after inoculation (Figure 2a, Supplemental Table S1). In the placebo group, nAB GMTs of 756 (median titers of 724) were detected seven days post-infection (Figure 2a). No nABs were found in the intact group, demonstrating that the inoculation of the virus had occurred in the W-PreS-O and placebo groups (Supplemental Table S1).

Preprints.org (www.preprints.org) | NOT PEER-REVIEWED | Posted: 29 May 2024 doi:10.20944/preprints202405.1895.v1

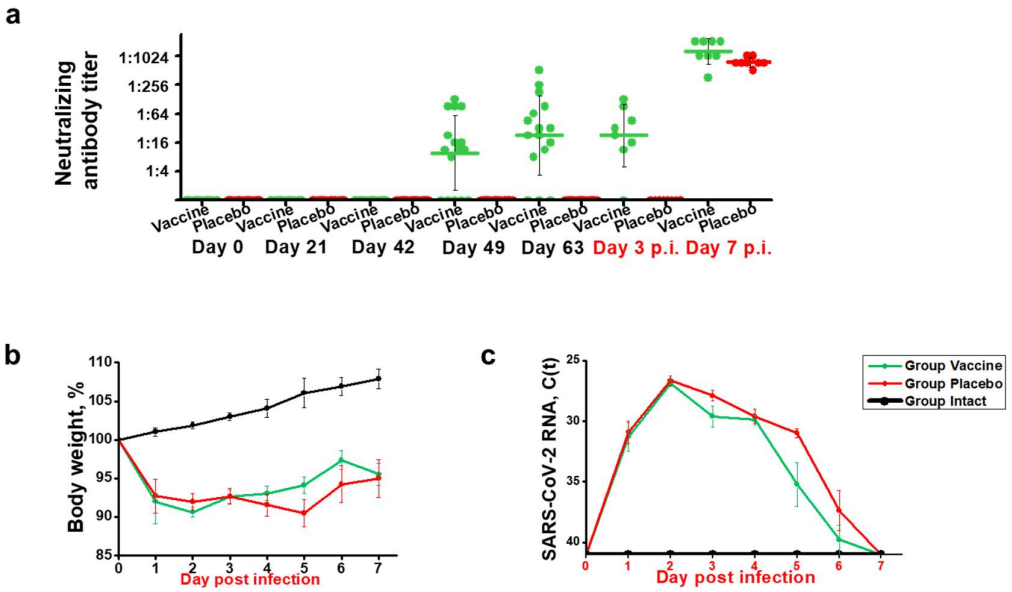

Figure 2. Neutralizing antibodies, body weight, and viral RNA load in oropharyngeal samples in Syrian hamsters. **(a)** Neutralizing antibody titers for the SARS-CoV-2 variant Omicron in sera (shown as a serum dilution, y-axis) were obtained at the indicated time points during immunization and after infection with virus. Titers below 1:8 were considered negative. Horizontal bars represent GMT values for each group (Green: vaccinated; red: placebo; black: not infected=intact). The dots are results for each animal and the whiskers indicate standard deviations. **(b)** Weight curves are presented as percentages of body weight before infection (y-axis) and **(c)** viral RNA contents in oropharyngeal swabs as cycle threshold C(t) values (y-axis) on the indicated days post-infection. C(t) values >40 were considered negative. The results are shown as mean values per group and standard deviations.

3.2. Recovery after SARS-CoV-2 Infection was Faster in Animals Immunized with W-PreS-O than in Placebo-Treated Animals

Hamsters are a non-lethal infection model for SARS-CoV-2 Omicron infections and COVID-19. After infection via the nasal route, the replication of SARS-CoV-2 in the respiratory tract yields pneumonia with inflammatory lesions in lungs on day 3 post-infection. Clinical signs observed in the animals after infection include weight loss and decrease in activity, and usually these symptoms resolve by 7–10 days after infection. In order to monitor the infection and study the clinical signs in animals immunized with the vaccine and placebo, the SARS-CoV-2 RNA load was detected in oropharyngeal samples, and the body weight was measured daily for seven days post-infection. Non-treated and non-infected animals (intact group) served as controls.

Infected animals from both groups treated with either W-PreS-O vaccine or placebo showed weight loss after challenge with SARS-CoV-2, in comparison with animals from the intact group, in the first three days after infection (Figure 2b). Of note, animals vaccinated with W-PreS-O started to gain weight 3 days post-infection, whereas animals from the placebo group started to gain weight 5 days after infection (Figure 2b). The viral load determined using the oropharyngeal swabs in the two groups showed similar results. C(t) values were 26.8 and 26.4 for the vaccine- and placebo-treated animals two days after infection, respectively (Figure 2c). On day five, the C(t) values in the vaccine group were median C(t) value 34.2, min: 29.5, max: 40, and in the placebo-treated group, median C(t) value 31, min: 28.9, max: 32.4, but there was no statistically significant difference on day five (Figure 2c).

3.3. Effects of Vaccination with W-PreS-O on Viral Loads in the Upper and Lower Respiratory Tract and Presence of Infectious Virus in the Lungs of Infected Animals

In the next set of experiments, we analyzed the viral load in the lungs of the animals using RT-PCR, and we then determined the titers of the infectious virus in the lungs. Finally, we assessed the viral RNA load using RT-PCR in the nasal cavities of the animals. On day 3 after infection, the SARS-CoV-2 RNA load in the lungs was slightly higher in the animals immunized with the W-PreS-O

Preprints.org (www.preprints.org) | NOT PEER-REVIEWED | Posted: 29 May 2024 doi:10.20944/preprints202405.1895.v1

vaccine than in the placebos (median C(t)-value vaccine: 20.3, placebo: 23.3), while seven days after infection, the viral loads were lower in the vaccinated than in the placebo group (median C(t)-value vaccine: 31.0, placebo: 28.8) (Figure 3a). However, there were no statistically significant differences between the W-PreS-O- and placebo-immunized animals in terms of viral RNA loads.

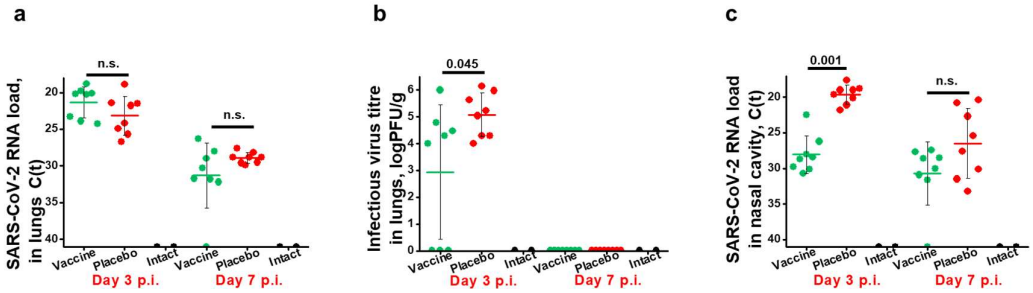

Figure 3. Effect of vaccination with recombinant fusion protein W-PreS-O on SARS-CoV-2 RNA loads in the lungs, infectious virus titers in the lungs, and SARS-CoV-2 RNA loads in the nasal cavities. **(a)** Viral RNA loads and **(b)** infectious virus titers in the lungs or **(c)** viral RNA loads in the nasal cavities of Syrian hamsters (y-axes) immunized three times with the W-PreS-O vaccine (green) or alum (placebo) (red) at the indicated time points after infection (x-axes) with SARS-CoV-2 variant Omicron. Untreated and non-infected animals (intact) (black) served as controls. Viral loads are given as cycle threshold C(t) values, and were considered negative if >40. Infectious virus titers, determined via plaque titration assay, are presented as logPFU/g values. The results are shown for individual animals, with horizontal bars representing mean values and whiskers indicating standard deviations per group (n = 8). Significant differences ($p < 0.05$) were determined with the Mann–Whitney test and are indicated. n.s.—not significant.

However, different results were obtained when the infectious virus titers in the lungs were measured. The animals vaccinated with W-PreS-O showed significantly lower infectious virus titers in the lungs (median log PFU/g lung: 4.1, min: 0, max: 6) than the animals immunized with placebo (median log PFU/g lung: 5.1, min: 4, max: 6) three days post-infection (Figure 3b). Of note, three out of the eight animals in the vaccine group had cleared the infectious virus from the lung tissue already by day three post-infection (Figure 3b). Notably, on day 3 post-infection, only vaccinated animals, and not placebo-treated animals, had developed nABs (Figure 2a). On day seven post-infection, infected animals from both the vaccinated and placebo groups had no infectious virus in the lungs anymore. At this time point, both groups had developed nABs (Figure 2a).

Finally, we investigated the viral load in the nasal cavities (i.e., the upper respiratory tract) of the animals (Figure 3c). Unlike in the lungs, we found that, on day three after infection, the animals vaccinated with W-PreS-O had a significantly reduced viral RNA load in the nasal cavities (median C(t) value: 28.6, min: 22.5, max: 30.7) as compared to placebo-immunized animals (median C(t) value: 19.3, min: 17.7, max: 21.8) (Figure 3c). This difference was highly significant (p=0.001). This result is consistent with the finding that neutralizing antibodies were present in the vaccinated but not in the placebo group on day 3 (Figure 2a). In the W-PreS-O immunized group, two out of eight animals (25%) had C(t) values above 30, and four out of the eight animals (50%) had C(t) values > 28, suggesting that that the animals were not infectious three days post-infection. On day 7 after infection, the mean C(t) value for the vaccinated animals was below 30 cycles, whereas the placebo-treated animals had a mean C(t) value of approximately 27 (Figure 3c), although the difference was not statistically significant.

3.4. Immunization with W-PreS-O Strongly Protects against Lung Damage

Next, we aimed to investigate the effects of vaccination with W-PreS-O on Omicron-induced lung damage by comparing edema formation and pneumonia indices in animals from the vaccine group and placebo group. Untreated and uninfected animals (intact group) served as the controls. Edema was estimated as the lung-to-body-weight ratio (Figure 4a). Lung edema was highest in the placebo group 3 and 7 d.p.i. as compared to the W-PreS-O-vaccinated animals and the intact group (Figure 4a). At 7 d.p.i., the edema in the placebo group was significantly worse than in the intact group. There were no significant differences in edema between the W-PreS-O immunized (vaccine)

Preprints.org (www.preprints.org) | NOT PEER-REVIEWED | Posted: 29 May 2024 doi:10.20944/preprints202405.1895.v1

and untreated, uninfected animals (intact) at three and seven days post-infection, respectively (Figure 4a).

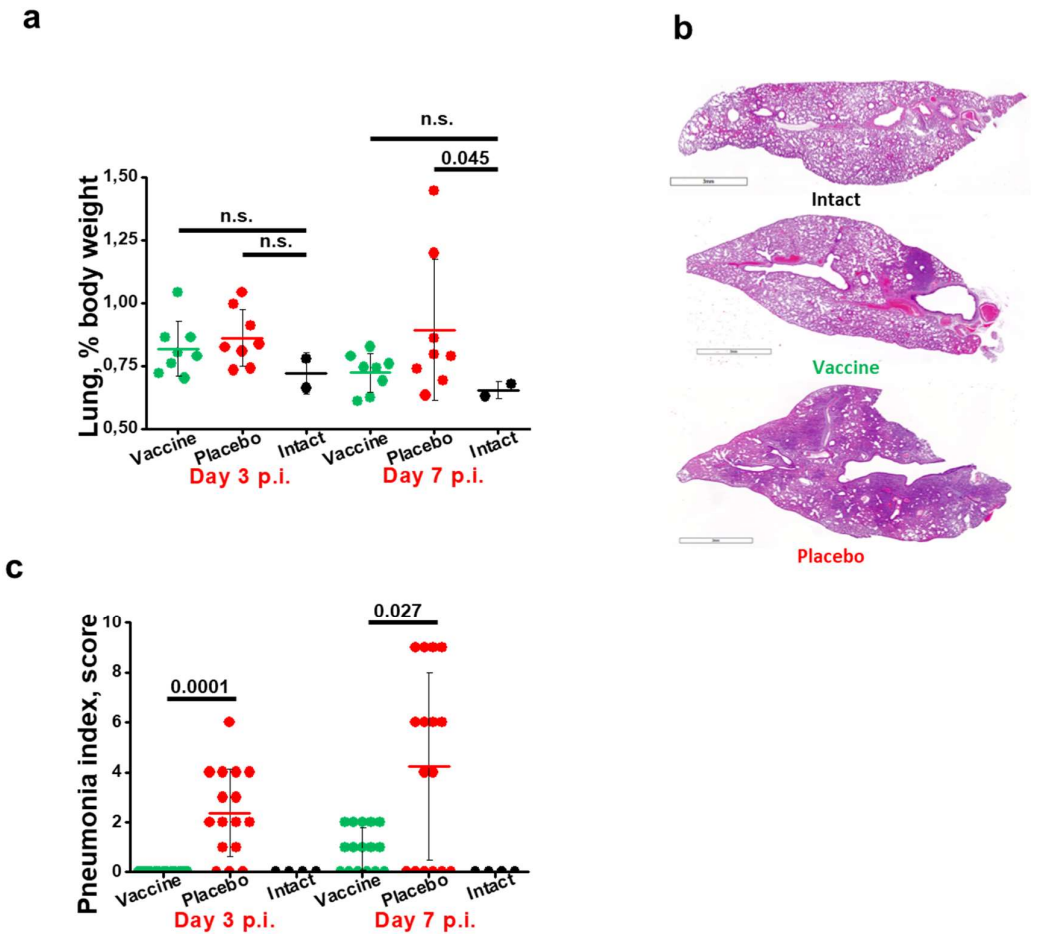

Figure 4. Severity of lung lesions in the different groups of infected animals. Pneumonia-caused lung edema is presented as **(a)** the weight coefficient of the total body weight (y-axis). Histological assessment of pneumonia severity is presented in **(b)** as representative microphotographs (lines indicate 3 mm) and **(c)** pneumonia indices (y-axis). The results are shown for individual sections and were calculated from semi-quantitative scores of the lesion area and pneumonia intensity for each section of investigated lung (two sections per animal). Results are shown for individual animals, with horizontal bars representing mean values and whiskers corresponding to standard deviations per group. Significant differences ($p < 0.05$) were determined with the Mann–Whitney test and are indicated. n.s.—not significant.

Lung tissue samples of animals from the W-PreS-O immunized group (vaccine) showed signs of antigenic stimulation three days post-infection, but no signs of pneumonia were observed (Figure 4b, Table S2), whereas the placebo group animals showed morphological signs of viral pneumonia of varying intensity, from mild bronchitis and incipient pneumonia (bronchopneumonia) to severe viral pneumonia with a characteristic hemorrhagic component and the presence of fibrinous exudate in the alveoli (Figure 4b, Table S2). As exemplified in Figure 4b and Table S2, the lungs from W-PreS-O-vaccinated animals showed some changes of varying intensity at 7 d.p.i., but the severity of these processes was much less pronounced than in the placebo group (Figure 4b, c). In fact, at 3 d.p.i., there was no evidence of pneumonia in the lungs of the W-PreS-O-vaccinated animals, which looked like the lungs from the uninfected hamsters (intact group). Thus, there was a highly significant difference in the pneumonia indices as compared to the placebo-treated animals on day 3 p.i. (p=0.0001) (Figure 4c). On day 7 p.i., the pneumonia indices in the W-PreS-O-vaccinated hamsters were very low and the difference, as compared to the placebo group, remained significant (Figure 4c, p=0.027).

Preprints.org (www.preprints.org) | NOT PEER-REVIEWED | Posted: 29 May 2024 doi:10.20944/preprints202405.1895.v1

4. Discussion

We previously developed a SARS-CoV-2 vaccine based on a recombinant fusion protein consisting of HBV-derived PreS with two flanking RBDs from the Wuhan strain, which induced high levels of neutralizing antibodies against the SARS-CoV-2 variants Alpha to Delta [42]. The goal of this study was to refine our vaccine platform for the Omicron variants. For this purpose, we compared the original fusion protein with one containing two Omicron RBDs, a mix of the original Wuhan-only fusion protein and the Omicron fusion protein, and a chimeric protein containing one RBD from Wuhan and one from Omicron (W-PreS-O) [24]. While the antibody levels induced in RBD from Wuhan and Omicron in mice by the four vaccine formulations were comparable, W-PreS-O induced considerably higher nAbs against the Omicron virus variant. We therefore selected W-PreS-O as a candidate vaccine to investigate for its ability to protect against Omicron in the Syrian hamster model [24]. In our study, a protective effect of the vaccine was clearly demonstrated by a significant reduction in infectious virus titers in the lungs in vaccinated versus placebo-treated animals, as demonstrated by measuring the infectious virus titers on day 3 (see Figure 3b). Second, the viral load in the nasal cavity was significantly reduced in vaccinated versus placebo-treated animals on day 3 after infection (see Figure 3c). Finally and importantly, immunization with W-PreS-O significantly reduced lung damage as compared to placebo immunization (see Figure 4c).

Several additional interesting findings were obtained from the Syrian hamster model when we compared animals vaccinated with W-PreS-O with animals that received placebo. The W-PreS-O-vaccinated animals developed robust nAb responses for Omicron after the last injection as compared to the placebo group. Interestingly, the nAb response in the W-PreS-O-vaccinated animals was strongly enhanced by natural infection with Omicron. In the vaccinated group, all but one animal, which already had a nAb titer of 512, increased their nAb titers to 1024 or higher, while only two out of eight animals in the placebo group reached a titer of 1024 through natural infection by 7 days after inoculation. This might be explained by the fact that vaccination with W-PreS-O had established a broad repertoire of Omicron RBD-specific T cells and B cells, which could be readily boosted by the natural infection. The W-PreS-O vaccine contains a W-PreS-O fusion protein displaying the RBD of Wuhan and Omicron as a naturally folded protein mimicking the fold of RBD in the virus [24]. The fact that secondary B cell memory in vaccinated animals could be strongly boosted by natural infection suggests that secondary T cells (i.e., $CD4^+$ and $CD8^+$) responses, which are also critically involved in protection, were boosted. However, this was not investigated in our study because the induction of protective antibody responses and the effects of vaccination versus placebo on lung pathology were the major endpoints of this study.

W-PreS-O-vaccinated animals showed a faster weight gain and physical recovery from infection than placebo-treated animals, but the difference was not significant as for other studies performed in Syrian hamsters infected with Omicron [46-48]. Of note, non-infected animals, which had not received any vaccinations, showed an approximately 7–10% greater gain of body weight than W-PreS-O- and placebo-vaccinated animals, indicating that the immunization process might have affected weight gain (Figure 2b).

The lung is the critical organ in COVID-19, and we therefore carefully studied the protective effects of vaccination with W-PreS-O against Omicron infection in the lower respiratory tract. Analysis of the presence of viral RNA in the lungs of W-PreS-O- and placebo-vaccinated animals found no significant differences between the groups (Figure 3a). However, when we studied the infectious virus loads in the lung via determining the infectious virus titers in lung tissue, we found a significant reduction in the W-PreS-O-vaccinated group as compared to the placebo group on day 3 after virus inoculation (Figure 3b). On day 7 after infection, no infectious virus was detected in either the W-PreS-O or placebo-treated animals. The results regarding the significantly reduced infectious virus loads in the lungs can be explained by the presence of nAbs in the vaccinated animals. When nAbs were elevated in the animals, infectious virus titers in the lungs were low (e.g., vaccinated group on day 3 after infection, Figures 2a, Figure 3b). When nAbs exceeded a certain threshold (e.g., vaccinated and placebo 7 days after infection, Figures 2a, 3b), no infectious virus was found in the lungs, likely because the nAbs had fully occupied the viral RBDs. The importance of generating nAbs by vaccination with W-PreS-O for protection against lung damage was demonstrated by a detailed histological investigation of the lung tissues (Figure 4). No significant edema was found in the W-PreS-O-vaccinated animals as compared to the non-infected (intact) hamsters (Figure 4a), and there

Preprints.org (www.preprints.org) | NOT PEER-REVIEWED | Posted: 29 May 2024 doi:10.20944/preprints202405.1895.v1

were almost no lung lesions, as demonstrated by the histology and pneumonia indexes, in the W-PreS-O-vaccinated animals. In contrast, the placebo-treated animals showed lung edema and elevated pneumonia indices at 3 and 7 days after infection (Figures 4b, c).

The Omicron infection model in Syrian hamsters is a complex in vivo model that may vary due to many different factors among studies. Nevertheless, many studies have been performed with licensed vaccines to study their effect on Omicron infections in Syrian hamsters. Several SARS-CoV-2 vaccines, combinations thereof, and different schedules and dose regimens of vaccination with these vaccines have been tested. It is impossible to compare all these vaccines, combinations, and schedules with our vaccine in one Syrian hamster experiment. However, to allow some comparison with our results, we considered infectious viral loads in the lungs because this parameter was assessed in most of the studies.

One study was performed with ChAdOx1 nCoV-19 (AZD1222), a replication-deficient simian adenovirus vector-based vaccine encoding the S protein from Wuhan-1, and AZD2816, encoding the S protein of the SARS-CoV-2 variant of concern Beta. This study showed a reduction in TCID50/g lung tissue as compared to the control vector on day 3, but the differences were not significant between vaccines and the placebo. [49]. A study investigating the efficacy of a vaccine based on a recombinant Omicron-derived S protein showed a significant reduction in infectious virus titers in the lungs of the Omicron-infected Syrian hamsters on day 3 compared to placebo. These results seemed to be comparable with ours [46]. Another study focused on the possible protective effect of booster vaccinations with licensed mRNA vaccines on Omicron infections in hamsters. This study showed that two, but not one, injection led to a modest reduction in infectious virus titers in the lungs [50]. Another study that performed an analysis on days 2 and 4 showed that two to three vaccinations with a heterologous vaccination regimen were able to reduce the infectious virus in the lungs, as we observed in our study. This was not achieved with a homologous vaccination regimen with three applications of the mRNA vaccine BNT162b on day 2, but a significant result was obtained by day 4 [47]. Finally, an interesting result was obtained for Covaxin^{R}, an inactivated SARS-CoV-2 whole virion vaccine, which reduced the viral load in the lung tissue after three doses three days after the hamsters were challenged with BA.2, while no effect for BA.1.1 was observed [51]. Taken together, it seems that the W-PreS-O vaccine has a protective effect against Omicron infections in the lungs of Syrian hamsters that is comparable or superior to that of currently licensed SARS-CoV-2 vaccines. Results obtained for the lungs are important in order to evaluate the effects of a SARS-CoV-2 vaccine on lung damage in the course of COVID-19.

It is also interesting to determine the viral loads in the upper respiratory tract to estimate the possible infectiousness of vaccinated animals. Such data may be obtained via the co-housing of vaccinated and infected animals with naïve animals, which was beyond the scope of our study. However, we analyzed the Omicron loads in the nasal cavities of the infected animal using RT-PCR. We found that the cycle thresholds for W-PreS-O-vaccinated animals were close to or above those considered to be infectious on day three after infection, whereas those in the placebo-treated animals were in the fully infectious range [52]. This result suggests that vaccination with W-PreS-O may induce, to some extent, sterilizing immunity.

In summary, W-PreS-O seems to be a highly promising SARS-CoV-2 subunit vaccine, and it should be further evaluated in clinical trials. Such clinical trials should investigate the ability of W-PreS-O to boost a predefined nAb response to currently circulating Omicron variants.

5. Conclusions

We found that the chimeric subunit vaccine W-PreS-O had protective effects against in vivo Omicron infection in the Syrian hamster model, which is the most commonly used in vivo model for SARS-CoV-2 infections. The key parameters of protection were as follows: (i.) vaccinated animals showed significantly reduced lung damage as compared to placebo-treated animals; (ii.) a significant reduction in infectious virus titers in the lungs of vaccinated versus placebo-treated animals was demonstrated; and (iii.) the viral load in the nasal cavity of vaccinated animals was significantly reduced compared to in the placebo group. Thus, W-PreS-O is a highly promising SARS-CoV-2 subunit vaccine for Omicron.

Preprints.org (www.preprints.org) | NOT PEER-REVIEWED | Posted: 29 May 2024 doi:10.20944/preprints202405.1895.v1

Supplementary Materials: The following supporting information can be downloaded at the website of this paper posted on Preprints.org. Figure S1. Sequence alignment of wild-type RBD and Omicron BA.1 and Omicron BA.1 strain 7995o. Table S1. Figure S2. Amino acid sequence of fusion protein W-PreS-O. SARS-CoV-2 Omicron-neutralizing antibody titers. Table S2. Histological examination of the lungs of experimental animals.

Author Contributions: Conceptualization, P.G., L.I.K., I.V.G., and R.V.; methodology, P.G. and L.I.K.; investigation, A.S.L., O.S.G., D.I.S., V.D.A., and E.S.C.; writing—original draft preparation, P.G., L.I.K., and R.V.; writing—review and editing, P.G., L.I.K., I.V.G., A.V.K., R.V., and A.A.I; visualization, P.G. and L.I.K.; supervision, R.V.; funding acquisition, R.V. and A.A.I. All authors have read and agreed to the published version of the manuscript.

Institutional Review Board Statement: The animal study protocol was approved by the Ethics Committee of the Chumakov FSC R&D IBP RAS (Protocol 190722-2 dated 19.06.22).

Data Availability Statement: The data presented in this study are available on request from the corresponding author.

Conflicts of Interest: R.V. has received research grants from HVD Life-Sciences, Vienna, Austria, WORG Pharmaceuticals, Hangzhou, China and from Viravaxx AG, Vienna, Austria. He serves as consultant for Viravaxx AG. R.V. and P.G. are authors on a patent application regarding the vaccine. The other authors have no conflicts of interest to declare. The funders had no role in the design of the study; in the collection, analyses, or interpretation of data; in the writing of the manuscript; or in the decision to publish the results. The authors with Russian affiliation declare that they have prepared the article in their "personal capacity" and/or that they are employed at an academic/research institution where research or education is the primary function of the entity.

References

1. Guan, W.J.; Ni, Z.Y.; Hu, Y.; Liang, W.H.; Ou, C.Q.; He, J.X.; Liu, L.; Shan, H.; Lei, C.L.; Hui, D.S.C.; et al. Clinical Characteristics of Coronavirus Disease 2019 in China. *N Engl J Med* **2020**, *382*, 1708-1720, doi:10.1056/NEJMoa2002032.
2. Dong, X.; Cao, Y.Y.; Lu, X.X.; Zhang, J.J.; Du, H.; Yan, Y.Q.; Akdis, C.A.; Gao, Y.D. Eleven faces of coronavirus disease 2019. *Allergy* **2020**, *75*, 1699-1709, doi:10.1111/all.14289.
3. Nesteruk, I. Endemic characteristics of SARS-CoV-2 infection. *Sci Rep* **2023**, *13*, 14841, doi:10.1038/s41598-023-41841-8.
4. Wrenn, J.O.; Pakala, S.B.; Vestal, G.; Shilts, M.H.; Brown, H.M.; Bowen, S.M.; Strickland, B.A.; Williams, T.; Mallal, S.A.; Jones, I.D.; et al. COVID-19 severity from Omicron and Delta SARS-CoV-2 variants. *Influenza Other Respir Viruses* **2022**, *16*, 832-836, doi:10.1111/irv.12982.
5. Menni, C.; Valdes, A.M.; Polidori, L.; Antonelli, M.; Penamakuri, S.; Nogal, A.; Louca, P.; May, A.; Figueiredo, J.C.; Hu, C.; et al. Symptom prevalence, duration, and risk of hospital admission in individuals infected with SARS-CoV-2 during periods of omicron and delta variant dominance: a prospective observational study from the ZOE COVID Study. *Lancet* **2022**, *399*, 1618-1624, doi:10.1016/s0140-6736(22)00327-0.
6. Fericean, R.M.; Oancea, C.; Reddyreddy, A.R.; Rosca, O.; Bratosin, F.; Bloanca, V.; Citu, C.; Alambaram, S.; Vasamsetti, N.G.; Dumitru, C. Outcomes of Elderly Patients Hospitalized with the SARS-CoV-2 Omicron B.1.1.529 Variant: A Systematic Review. *Int J Environ Res Public Health* **2023**, *20*, doi:10.3390/ijerph20032150.
7. Nori, W.; Ghani Zghair, M.A. Omicron targets upper airways in pediatrics, elderly and unvaccinated population. *World J Clin Cases* **2022**, *10*, 12062-12065, doi:10.12998/wjcc.v10.i32.12062.
8. Chen, X.; Wang, H.; Ai, J.; Shen, L.; Lin, K.; Yuan, G.; Sheng, X.; Jin, X.; Deng, Z.; Xu, J.; et al. Identification of CKD, bedridden history and cancer as higher-risk comorbidities and their impact on prognosis of hospitalized Omicron patients: a multi-centre cohort study. *Emerg Microbes Infect* **2022**, *11*, 2501-2509, doi:10.1080/22221751.2022.2122581.
9. Mongin, D.; Bürgisser, N.; Laurie, G.; Schimmel, G.; Vu, D.L.; Cullati, S.; Courvoisier, D.S. Effect of SARS-CoV-2 prior infection and mRNA vaccination on contagiousness and susceptibility to infection. *Nat Commun* **2023**, *14*, 5452, doi:10.1038/s41467-023-41109-9.
10. Bobrovitz, N.; Ware, H.; Ma, X.; Li, Z.; Hosseini, R.; Cao, C.; Selemon, A.; Whelan, M.; Premji, Z.; Issa, H.; et al. Protective effectiveness of previous SARS-CoV-2 infection and hybrid immunity against the omicron variant and severe disease: a systematic review and meta-regression. *Lancet Infect Dis* **2023**, *23*, 556-567, doi:10.1016/s1473-3099(22)00801-5.
11. Tian, D.; Sun, Y.; Xu, H.; Ye, Q. The emergence and epidemic characteristics of the highly mutated SARS-CoV-2 Omicron variant. *J Med Virol* **2022**, *94*, 2376-2383, doi:10.1002/jmv.27643.
12. Shrestha, L.B.; Foster, C.; Rawlinson, W.; Tedla, N.; Bull, R.A. Evolution of the SARS-CoV-2 omicron variants BA.1 to BA.5: Implications for immune escape and transmission. *Rev Med Virol* **2022**, *32*, e2381, doi:10.1002/rmv.2381.

Preprints.org (www.preprints.org) | NOT PEER-REVIEWED | Posted: 29 May 2024 doi:10.20944/preprints202405.1895.v1

13. Gattinger, P.; Tulaeva, I.; Borochova, K.; Kratzer, B.; Trapin, D.; Kropfmüller, A.; Pickl, W.F.; Valenta, R. Omicron: A SARS-CoV-2 variant of real concern. *Allergy* **2022**, *77*, 1616-1620, doi:10.1111/all.15264.
14. Uemura, K.; Kanata, T.; Ono, S.; Michihata, N.; Yasunaga, H. The disease severity of COVID-19 caused by Omicron variants: A brief review. *Ann Clin Epidemiol* **2023**, *5*, 31-36, doi:10.37737/ace.23005.
15. Garcia-Beltran, W.F.; St Denis, K.J.; Hoelzemer, A.; Lam, E.C.; Nitido, A.D.; Sheehan, M.L.; Berrios, C.; Ofoman, O.; Chang, C.C.; Hauser, B.M.; et al. mRNA-based COVID-19 vaccine boosters induce neutralizing immunity against SARS-CoV-2 Omicron variant. *Cell* **2022**, *185*, 457-466.e454, doi:10.1016/j.cell.2021.12.033.
16. Wolter, N.; Jassat, W.; Walaza, S.; Welch, R.; Moultrie, H.; Groome, M.; Amoako, D.G.; Everatt, J.; Bhiman, J.N.; Scheepers, C.; et al. Early assessment of the clinical severity of the SARS-CoV-2 omicron variant in South Africa: a data linkage study. *Lancet* **2022**, *399*, 437-446, doi:10.1016/s0140-6736(22)00017-4.
17. Cao, Y.; Jian, F.; Wang, J.; Yu, Y.; Song, W.; Yisimayi, A.; Wang, J.; An, R.; Chen, X.; Zhang, N.; et al. Imprinted SARS-CoV-2 humoral immunity induces convergent Omicron RBD evolution. *Nature* **2023**, *614*, 521-529, doi:10.1038/s41586-022-05644-7.
18. Chen, L.; He, Y.; Liu, H.; Shang, Y.; Guo, G. Potential immune evasion of the severe acute respiratory syndrome coronavirus 2 Omicron variants. *Front Immunol* **2024**, *15*, 1339660, doi:10.3389/fimmu.2024.1339660.
19. Alam, M.S. Insight into SARS-CoV-2 Omicron variant immune escape possibility and variant independent potential therapeutic opportunities. *Heliyon* **2023**, *9*, e13285, doi:10.1016/j.heliyon.2023.e13285.
20. Carabelli, A.M.; Peacock, T.P.; Thorne, L.G.; Harvey, W.T.; Hughes, J.; Peacock, S.J.; Barclay, W.S.; de Silva, T.I.; Towers, G.J.; Robertson, D.L. SARS-CoV-2 variant biology: immune escape, transmission and fitness. *Nat Rev Microbiol* **2023**, *21*, 162-177, doi:10.1038/s41579-022-00841-7.
21. Zak, A.J.; Hoang, T.; Yee, C.M.; Rizvi, S.M.; Prabhu, P.; Wen, F. Pseudotyping Improves the Yield of Functional SARS-CoV-2 Virus-like Particles (VLPs) as Tools for Vaccine and Therapeutic Development. *Int J Mol Sci* **2023**, *24*, doi:10.3390/ijms241914622.
22. Wang, R.; Huang, H.; Yu, C.; Sun, C.; Ma, J.; Kong, D.; Lin, Y.; Zhao, D.; Zhou, S.; Lu, J.; et al. A spike-trimer protein-based tetravalent COVID-19 vaccine elicits enhanced breadth of neutralization against SARS-CoV-2 Omicron subvariants and other variants. *Sci China Life Sci* **2023**, *66*, 1818-1830, doi:10.1007/s11427-022-2207-7.
23. Chau, E.C.T.; Kwong, T.C.; Pang, C.K.; Chan, L.T.; Chan, A.M.L.; Yao, X.; Tam, J.S.L.; Chan, S.W.; Leung, G.P.H.; Tai, W.C.S.; et al. A Novel Probiotic-Based Oral Vaccine against SARS-CoV-2 Omicron Variant B.1.1.529. *Int J Mol Sci* **2023**, *24*, doi:10.3390/ijms241813931.
24. Gattinger, P.; Kratzer, B.; Sehgal, A.N.A.; Ohradanova-Repic, A.; Gebetsberger, L.; Tajti, G.; Focke-Tejkl, M.; Schaar, M.; Fuhrmann, V.; Petrowitsch, L.; et al. Vaccine Based on Recombinant Fusion Protein Combining Hepatitis B Virus PreS with SARS-CoV-2 Wild-Type- and Omicron-Derived Receptor Binding Domain Strongly Induces Omicron-Neutralizing Antibodies in a Murine Model. *Vaccines (Basel)* **2024**, *12*, doi:10.3390/vaccines12030229.
25. Blain, H.; Tuaillon, E.; Gamon, L.; Pisoni, A.; Miot, S.; Delpui, V.; Si-Mohamed, N.; Niel, C.; Rolland, Y.; Montes, B.; et al. Receptor binding domain-IgG levels correlate with protection in residents facing SARS-CoV-2 B.1.1.7 outbreaks. *Allergy* **2022**, *77*, 1885-1894, doi:10.1111/all.15142.
26. Gattinger, P.; Niespodziana, K.; Stiasny, K.; Sahanic, S.; Tulaeva, I.; Borochova, K.; Dorofeeva, Y.; Schlederer, T.; Sonnweber, T.; Hofer, G.; et al. Neutralization of SARS-CoV-2 requires antibodies against conformational receptor-binding domain epitopes. *Allergy* **2022**, *77*, 230-242, doi:10.1111/all.15066.
27. Gattinger, P.; Ohradanova-Repic, A.; Valenta, R. Importance, Applications and Features of Assays Measuring SARS-CoV-2 Neutralizing Antibodies. *Int J Mol Sci* **2023**, *24*, doi:10.3390/ijms24065352.
28. Rocha, V.P.C.; Quadros, H.C.; Fernandes, A.M.S.; Gonçalves, L.P.; Badaró, R.; Soares, M.B.P.; Machado, B.A.S. An Overview of the Conventional and Novel Methods Employed for SARS-CoV-2 Neutralizing Antibody Measurement. *Viruses* **2023**, *15*, doi:10.3390/v15071504.
29. Caldera-Crespo, L.A.; Paidas, M.J.; Roy, S.; Schulman, C.I.; Kenyon, N.S.; Daunert, S.; Jayakumar, A.R. Experimental Models of COVID-19. *Front Cell Infect Microbiol* **2021**, *11*, 792584, doi:10.3389/fcimb.2021.792584.
30. Davidson, M.K.; Lindsey, J.R.; Davis, J.K. Requirements and selection of an animal model. *Isr J Med Sci* **1987**, *23*, 551-555.
31. Miao, J.; Chard, L.S.; Wang, Z.; Wang, Y. Syrian Hamster as an Animal Model for the Study on Infectious Diseases. *Front Immunol* **2019**, *10*, 2329, doi:10.3389/fimmu.2019.02329.
32. Schaecher, S.R.; Stabenow, J.; Oberle, C.; Schriewer, J.; Buller, R.M.; Sagartz, J.E.; Pekosz, A. An immunosuppressed Syrian golden hamster model for SARS-CoV infection. *Virology* **2008**, *380*, 312-321, doi:10.1016/j.virol.2008.07.026.
33. Iwatsuki-Horimoto, K.; Nakajima, N.; Ichiko, Y.; Sakai-Tagawa, Y.; Noda, T.; Hasegawa, H.; Kawaoka, Y. Syrian Hamster as an Animal Model for the Study of Human Influenza Virus Infection. *J Virol* **2018**, *92*, doi:10.1128/jvi.01693-17.

Preprints.org (www.preprints.org) | NOT PEER-REVIEWED | Posted: 29 May 2024 doi:10.20944/preprints202405.1895.v1

34. Frere, J.J.; Serafini, R.A.; Pryce, K.D.; Zazhytska, M.; Oishi, K.; Golynker, I.; Panis, M.; Zimering, J.; Horiuchi, S.; Hoagland, D.A.; et al. SARS-CoV-2 infection in hamsters and humans results in lasting and unique systemic perturbations after recovery. *Sci Transl Med* **2022**, *14*, eabq3059, doi:10.1126/scitranslmed.abq3059.
35. Sia, S.F.; Yan, L.M.; Chin, A.W.H.; Fung, K.; Choy, K.T.; Wong, A.Y.L.; Kaewpreedee, P.; Perera, R.; Poon, L.L.M.; Nicholls, J.M.; et al. Pathogenesis and transmission of SARS-CoV-2 in golden hamsters. *Nature* **2020**, *583*, 834-838, doi:10.1038/s41586-020-2342-5.
36. Huang, C.; Wang, Y.; Li, X.; Ren, L.; Zhao, J.; Hu, Y.; Zhang, L.; Fan, G.; Xu, J.; Gu, X.; et al. Clinical features of patients infected with 2019 novel coronavirus in Wuhan, China. *Lancet* **2020**, *395*, 497-506, doi:10.1016/s0140-6736(20)30183-5.
37. Castellan, M.; Zamperin, G.; Franzoni, G.; Foiani, G.; Zorzan, M.; Drzewnioková, P.; Mancin, M.; Brian, I.; Bortolami, A.; Pagliari, M.; et al. Host Response of Syrian Hamster to SARS-CoV-2 Infection including Differences with Humans and between Sexes. *Viruses* **2023**, *15*, doi:10.3390/v15020428.
38. Chen, Z.; Yuan, Y.; Hu, Q.; Zhu, A.; Chen, F.; Li, S.; Guan, X.; Lv, C.; Tang, T.; He, Y.; et al. SARS-CoV-2 immunity in animal models. *Cell Mol Immunol* **2024**, *21*, 119-133, doi:10.1038/s41423-023-01122-w.
39. Halfmann, P.J.; Iida, S.; Iwatsuki-Horimoto, K.; Maemura, T.; Kiso, M.; Scheaffer, S.M.; Darling, T.L.; Joshi, A.; Loeber, S.; Singh, G.; et al. SARS-CoV-2 Omicron virus causes attenuated disease in mice and hamsters. *Nature* **2022**, *603*, 687-692, doi:10.1038/s41586-022-04441-6.
40. Yuan, S.; Ye, Z.W.; Liang, R.; Tang, K.; Zhang, A.J.; Lu, G.; Ong, C.P.; Man Poon, V.K.; Chan, C.C.; Mok, B.W.; et al. Pathogenicity, transmissibility, and fitness of SARS-CoV-2 Omicron in Syrian hamsters. *Science* **2022**, *377*, 428-433, doi:10.1126/science.abn8939.
41. Vogel, G. Omicron shots are coming-with lots of questions. *Science* **2022**, *377*, 1029-1030, doi:10.1126/science.ade6580.
42. Gattinger, P.; Kratzer, B.; Tulaeva, I.; Niespodziana, K.; Ohradanova-Repic, A.; Gebetsberger, L.; Borochova, K.; Garner-Spitzer, E.; Trapin, D.; Hofer, G.; et al. Vaccine based on folded receptor binding domain-PreS fusion protein with potential to induce sterilizing immunity to SARS-CoV-2 variants. *Allergy* **2022**, *77*, 2431-2445, doi:10.1111/all.15305.
43. Valenta, R.; Campana, R.; Niederberger, V. Recombinant allergy vaccines based on allergen-derived B cell epitopes. *Immunol Lett* **2017**, *189*, 19-26, doi:10.1016/j.imlet.2017.04.015.
44. Cornelius, C.; Schöneweis, K.; Georgi, F.; Weber, M.; Niederberger, V.; Zieglmayer, P.; Niespodziana, K.; Trauner, M.; Hofer, H.; Urban, S.; et al. Immunotherapy With the PreS-based Grass Pollen Allergy Vaccine BM32 Induces Antibody Responses Protecting Against Hepatitis B Infection. *EBioMedicine* **2016**, *11*, 58-67, doi:10.1016/j.ebiom.2016.07.023.
45. Kärber, G. Beitrag zur kollektiven Behandlung pharmakologischer Reihenversuche. *Naunyn-Schmiedebergs Archiv für experimentelle Pathologie und Pharmakologie* **1931**, *162*, 480-483, doi:10.1007/BF01863914.
46. Boon, J.; Soudani, N.; Bricker, T.; Darling, T.; Seehra, K.; Patel, N.; Guebre-Xabier, M.; Smith, G.; Suthar, M.; Ellebedy, A.; et al. Immunogenicity and efficacy of XBB.1.5 rS vaccine against EG.5.1 variant of SARS-CoV-2 in Syrian hamsters. *Res Sq* **2024**, doi:10.21203/rs.3.rs-3873514/v1.
47. Machado, R.R.G.; Walker, J.L.; Scharton, D.; Rafael, G.H.; Mitchell, B.M.; Reyna, R.A.; de Souza, W.M.; Liu, J.; Walker, D.H.; Plante, J.A.; et al. Immunogenicity and efficacy of vaccine boosters against SARS-CoV-2 Omicron subvariant BA.5 in male Syrian hamsters. *Nat Commun* **2023**, *14*, 4260, doi:10.1038/s41467-023-40033-2.
48. Zhou, B.; Zhou, R.; Tang, B.; Chan, J.F.; Luo, M.; Peng, Q.; Yuan, S.; Liu, H.; Mok, B.W.; Chen, B.; et al. A broadly neutralizing antibody protects Syrian hamsters against SARS-CoV-2 Omicron challenge. *Nat Commun* **2022**, *13*, 3589, doi:10.1038/s41467-022-31259-7.
49. van Doremalen, N.; Schulz, J.E.; Adney, D.R.; Saturday, T.A.; Fischer, R.J.; Yinda, C.K.; Thakur, N.; Newman, J.; Ulaszewska, M.; Belij-Rammerstorfer, S.; et al. ChAdOx1 nCoV-19 (AZD1222) or nCoV-19-Beta (AZD2816) protect Syrian hamsters against Beta Delta and Omicron variants. *Nat Commun* **2022**, *13*, 4610, doi:10.1038/s41467-022-32248-6.
50. Halfmann, P.J.; Uraki, R.; Kuroda, M.; Iwatsuki-Horimoto, K.; Yamayoshi, S.; Ito, M.; Kawaoka, Y. Transmission and re-infection of Omicron variant XBB.1.5 in hamsters. *EBioMedicine* **2023**, *93*, 104677, doi:10.1016/j.ebiom.2023.104677.
51. Yadav, P.D.; Mohandas, S.; Shete, A.; Sapkal, G.; Deshpande, G.; Kumar, A.; Wakchaure, K.; Dighe, H.; Jain, R.; Ganneru, B.; et al. Protective efficacy of COVAXIN® against Delta and Omicron variants in hamster model. *iScience* **2022**, *25*, 105178, doi:10.1016/j.isci.2022.105178.
52. Hay, J.A.; Kissler, S.M.; Fauver, J.R.; Mack, C.; Tai, C.G.; Samant, R.M.; Connolly, S.; Anderson, D.J.; Khullar, G.; MacKay, M.; et al. Quantifying the impact of immune history and variant on SARS-CoV-2 viral kinetics and infection rebound: A retrospective cohort study. *Elife* **2022**, *11*, doi:10.7554/eLife.81849.

Disclaimer/Publisher's Note: The statements, opinions and data contained in all publications are solely those of the individual author(s) and contributor(s) and not of MDPI and/or the editor(s). MDPI and/or the editor(s)

Preprints.org (www.preprints.org) | NOT PEER-REVIEWED | Posted: 29 May 2024 doi:10.20944/preprints202405.1895.v1

disclaim responsibility for any injury to people or property resulting from any ideas, methods, instructions or products referred to in the content.